Linear-response theory of the longitudinal spin Seebeck effect

Hiroto Adachi* and Sadamich Maekawa

Advanced Science Research Center, Japan Atomic Energy Agency, Tokai 319-1195, Japan

We theoretically investigate the *longitudinal* spin Seebeck effect, in which the spin current is injected from a ferromagnet into an attached nonmagnetic metal in a direction *parallel* to the temperature gradient. Using the fact that the phonon heat current flows intensely into the attached nonmagnetic metal in this particular configuration, we show that the sign of the spin injection signal in the longitudinal spin Seebeck effect can be opposite to that in the conventional transverse spin Seebeck effect when the electron-phonon interaction in the nonmagnetic metal is sufficiently large. Our linear-response approach can explain the sign reversal of the spin injection signal recently observed in the longitudinal spin Seebeck effect.
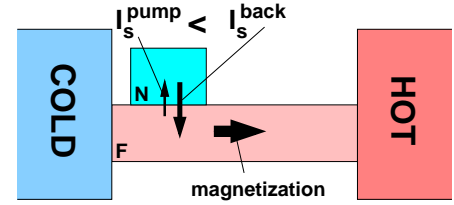
I. INTRODUCTION

Because of the desire to deal with heating problems in modern spintronic devices, there has been an increasing interest in investigating thermal effects in spintronics. A new subfield "spin caloritronics" [1] aims to understand the basic physics behind the interplay of spin and heat. One of the central issues in spin caloritronics is the newly discovered thermo-spin phenomenon termed spin Seebeck effect [2], which enables the thermal injection of spin currents from a ferromagnet into attached nonmagnetic metals over a macroscopic scale of several millimeters. The spin Seebeck effect is now established as a universal aspect of ferromagnets because this phenomenon is observed in various materials ranging from the metallic ferromagnets $Ni_{81}Fe_{19}$ [2] and Co_2MnSi [3], to the semiconducting ferromagnet (Ga,Mn)As [4], to the insulating magnets $LaY_2Fe_5O_{12}$ [5].

It is important to note that the above experiments [2–5] were performed in a configuration of the *transverse* spin Seebeck effect, in which the direction of the thermal spin injection into the attached nonmagnetic metal is *perpendicular* to the temperature gradient [Fig. 1 (a)]. Recently, another type of spin Seebeck effect called the *longitudinal* spin Seebeck effect [6, 7] is reported, in which the direction of the thermal spin injection into the nonmagnetic metal is *parallel* to the temperature gradient [Fig. 1 (b)]. Whereas the longitudinal spin Seebeck effect is well defined only for the use of an *insulating* ferromagnet due to the parasitic contribution from the anomalous Nernst effect [8, 9], it has several attractive features: (i) it is substrate free, (ii) the configuration is much simpler than that of the transverse spin Seebeck effect, and (iii) it can be of wide application because it allows the use of bulk samples.

Another pronounced feature of the longitudinal spin Seebeck effect is that the sign of the spin injection signal is opposite to that in the transverse spin Seebeck ef-
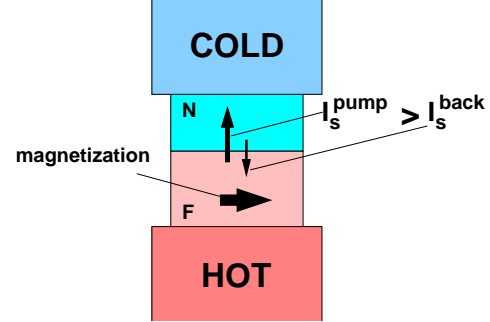
(a) Transverse

(b) Longitudinal

FIG. 1: (Color online) Schematic view of the experimental setup for (a) the transverse spin Seebeck effect and (b) the longitudinal spin Seebeck effect.

fect [6, 7]. Physically, the longitidinal spin Seebeck effect is distinguished from the transverse spin Seebeck effect by the fact that the attached nonmagnetic metal is in contact with the heat bath in the longitudinal setup, while the attached nonmagnetic metal is out of contact with the heat bath in the transverse setup. This brings about a clear difference that the heat current intensely flows into the attached nonmagnetic metal in the case of the longitudinal spin Seebeck effect, whereas it does not in the case of the transverse spin Seebeck effect. It is obvious that theory of magnon-driven spin Seebeck effect [10] fails to explain the situation in question.

In this paper, by employing linear-response theory of the spin Seebeck effect [11] and using the importance of

the phonon-drag process in the spin Seebeck effect [12], we show that the sign of the spin injection signal in the longitudinal spin Seebeck effect can be opposite to that in the conventional transverse spin Seebeck effect when the electron-phonon interaction in the attached nonmagnetic metal is sufficiently large. The key in our discussion is the aforementioned difference in the position of the attached nonmagnetic metal between the longitudinal setup and the transverse setup.

II. PHENOMENOLOGY OF THE LONGITUDINAL SPIN SEEBECK EFFECT

Let us begin with the phenomenology of the longitudinal spin Seebeck effect. In Fig. 1, a hybrid structure of a ferromagnet (F) and a nonmagnetic metal (N) is placed under a temperature gradient. The central quantity that characterizes the spin Seebeck effect is the spin current I_s injected into N. As explained in detail in Ref. [13], the spin Seebeck effect is a thermal spin injection by localized spins, and the injected spin current has two contributions,

$$I_s = I_s^{\mathrm{pump}} - I_s^{\mathrm{back}}, \qquad (1)$$

where I_s^{pump} (the so-called pumping component) represents the spin current pumped into N by the thermal fluctuations of localized spins in F, while I_s^{back} (the so-called backflow component) represents the spin current coming back into F by the thermal fluctuations of the spin accumulations in N. We now focus on the spin current injected into N which is located close to the *cold* reservoir. In the case of the conventional transverse spin Seebeck effect, the pumping component I_s^{pump} is lesser than the backflow component I_s^{pump} [Fig. 1(a)]. In contrast, I_s^{pump} is greater than the backflow component I_s^{pump} in the case of the longitudinal spin Seebeck effect [Fig. 1(b)].

This difference can be explained phenomenologically on the basis of the following conditions: (i) most of the heat current in the F/N hybrid system at room temperature is carried by phonons (see Ref. [14] in the case of yttrium iron garnet), and (ii) the interaction between the phonons and the spin accumulation in N is much stronger than the magnon-phonon interaction in F.

First, recall that the pumping and backflow components can be expressed as follows [13]:

$$I_s^{\mathrm{pump}} = -G_s k_B T_F^*, \qquad (2)$$
$$I_s^{\mathrm{back}} = -G_s k_B T_N^*, \qquad (3)$$

where T_F^* and T_N^* are the effective temperature of the magnon in F and the spin accumulation in N. Here, $G_s = J_{\mathrm{sd}}^2 \chi_N \tau_{\mathrm{sf}}/\hbar$ with J_{sd}, χ_N, and τ_{sf} being the s-d interaction at the interface, the paramagnetic susceptibility in N, and the spin diffusion length in N, respectively. The negative sign before G_s arises from the fact that the magnon carries spin -1. In the longitudinal spin Seebeck experiment, the nonmagnetic metal N is in direct contact with the heat bath, and thereby is exposed to the flow of the phonon heat current due to condition (i). Then, because of condition (ii), spin accumulation in N is heated up faster than the magnons in the ferromagnet F, and the resultant effective temperature of the spin accumulation in N increases above that of the magnons in F. In the conventional transverse spin Seebeck setup, by contrast, the nonmagnetic metal N is out of contact with the heat bath and the phonon heat current does not flow through the nonmagnetic metal N, while the ferromagnet F is in contact with the heat bath, resulting in an increase in the effective magnon temperature in F. Therefore, in this case, the effective temperature of the spin accumulation in N is lower than that of the magnons in F. This difference can explain the sign reversal of the spin Seebeck effect signal between the longitudinal setup and the conventional transverse setup.

III. LINEAR-RESPONSE FORMULATION

In this section we review the linear-response formalism of the spin Seebeck effect developed in Ref. [11]. In the next section, this formalism is employed to evaluate the longitudinal spin Seebeck effect. We use a model shown in Fig. 2, in which the localized spins in F are interacting with the spin accumulation in N through the s-d exchange interaction J_{sd} at the interface. In our approach, the spin accumulation is modeled as a nonequilibrium itinerant spin density $\boldsymbol{s}$.

As in Ref. [11], the spin current I_s injected into the nonmagnetic metal N is calculated as $I_s(t) = -\sum_{\boldsymbol{q},\boldsymbol{k}} \frac{4\mathcal{J}_{\mathrm{sd}}^{\boldsymbol{k}+\boldsymbol{q}}\sqrt{S_0}}{\sqrt{2N_F N_N}\hbar} \mathrm{Re} C_{\boldsymbol{k},\boldsymbol{q}}^<(t,t)$, where N_F (N_N) is the number of lattice sites in F (N), S_0 is the size of the localized spins in F, and $\mathcal{J}_{\mathrm{sd}}^{\boldsymbol{k}+\boldsymbol{q}}$ is the Fourier transform of the s-d interaction at the F/N interface. Here, $C_{\boldsymbol{k},\boldsymbol{q}}^<(t,t') = -\mathrm{i}\langle a_{\boldsymbol{q}}^+(t') s_{\boldsymbol{k}}^-(t)\rangle$ measures the correlation between the magnon operator $a_{\boldsymbol{q}}^+$ in F and the itinerant spin-density operator $s_{\boldsymbol{k}}^- = (s_{\boldsymbol{k}}^x - \mathrm{i}s_{\boldsymbol{k}}^y)/2$ in N. Note that the time dependence of $I_s(t)$ vanishes in the steady state and it is hereafter discarded. Introducing the frequency representation $C_{\boldsymbol{k},\boldsymbol{q}}^<(t-t') = \int_{-\infty}^{\infty} \frac{d\omega}{2\pi} C_{\boldsymbol{q},\boldsymbol{k}}^<(\omega) e^{-\mathrm{i}\omega(t-t')}$ and adopting the representation [15] $\check{C} = \begin{pmatrix} C^R, C^K \\ 0, C^A \end{pmatrix}$ as well as using the relation $C^< = \frac{1}{2}[C^K - C^R + C^A]$, we obtain

$$I_s = \sum_{\boldsymbol{q},\boldsymbol{k}} \frac{-2\mathcal{J}_{\mathrm{sd}}^{\boldsymbol{k}-\boldsymbol{q}}\sqrt{S_0}}{\sqrt{2N_F N_N}\hbar} \int_{-\infty}^{\infty} \frac{d\omega}{2\pi} \mathrm{Re} C_{\boldsymbol{k},\boldsymbol{q}}^K(\omega) \qquad (4)$$

for the spin current I_s in the steady state [16].

Up to the lowest order in the s-d interaction J_{sd}, the interface correlation function $\check{C}$ appearing in Eq. (4) is generally expressed as

$$\check{C}_{\boldsymbol{k},\boldsymbol{q}}(\omega) = \frac{\mathcal{J}_{\mathrm{sd}}^{\boldsymbol{k}-\boldsymbol{q}}\sqrt{S_0}}{\sqrt{N_N N_F}\hbar} \underline{\check{\chi}}_{\boldsymbol{k}}(\omega) \underline{\check{X}}_{\boldsymbol{q}}(\omega), \qquad (5)$$
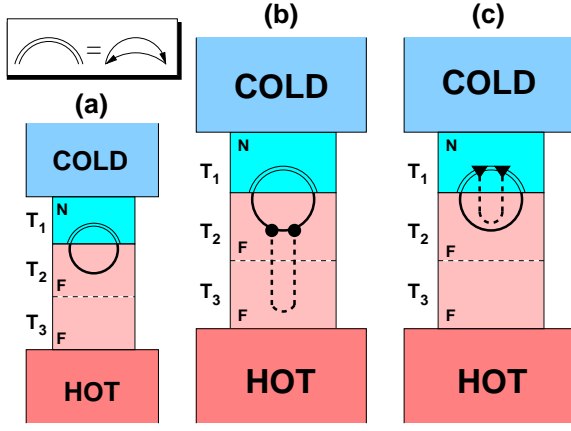
FIG. 2: (Color online) Diagrammatic representation of the spin Seebeck effect in the longitudinal configuration. The double solid line (the dashed line) represents the propagator of the itinerant spin density (the phonon). The solid circle (solid triangle) denotes the interaction vertex $\Gamma_{K,q}$ ($\Upsilon_{K,k}$) between the magnon and the phonon (the itinerant spin density and the phonon). Here, $T_1 < T_2 < T_3$.

where $\underline{\check{X}}_{\boldsymbol{q}}(\omega) = \check{X}_{\boldsymbol{q}}(\omega) + \delta\check{X}_{\boldsymbol{q}}(\omega)$ is the renormalized magnon propagator with the bare component $\check{X}_{\boldsymbol{q}}(\omega)$, and $\underline{\check{\chi}}_{\boldsymbol{k}}(\omega) = \check{\chi}_{\boldsymbol{k}}(\omega) + \delta\check{\chi}_{\boldsymbol{k}}(\omega)$ is the renormalized spin-density propagator with the bare component $\check{\chi}_{\boldsymbol{k}}(\omega)$. The bare magnon propagator satisfies the equilibrium condition:

$$X_{\boldsymbol{q}}^A(\omega) = [X_{\boldsymbol{q}}^R(\omega)]^*, \quad X_{\boldsymbol{q}}^K(\omega) = 2i\,\mathrm{Im}X_{\boldsymbol{q}}^R(\omega)\coth(\tfrac{\hbar\omega}{2k_\mathrm{B}T}), \tag{6}$$

where the retarded component is given by $X_{\boldsymbol{q}}^R(\omega) = (\omega - \widetilde{\omega}_{\boldsymbol{q}} + i\alpha\omega)^{-1}$ with $\widetilde{\omega}_{\boldsymbol{q}} = \gamma H_0 + \omega_{\boldsymbol{q}}$ being the magnon frequency for uniform mode γH_0 and exchange mode $\omega_{\boldsymbol{q}} = D_\mathrm{ex}q^2/\hbar$. Likewise, the bare spin-density propagator satisfies the local equilibrium condition:

$$\chi_{\boldsymbol{k}}^A(\omega) = [\chi_{\boldsymbol{k}}^R(\omega)]^*, \quad \chi_{\boldsymbol{k}}^K(\omega) = 2i\,\mathrm{Im}\chi_{\boldsymbol{k}}^R(\omega)\coth(\tfrac{\hbar\omega}{2k_\mathrm{B}T}), \tag{7}$$

where the retarded component of $\check{\chi}_{\boldsymbol{k}}(\omega)$ is given by $\chi_{\boldsymbol{k}}^R(\omega) = \chi_N/(1 + \lambda_\mathrm{sf}^2 k^2 - i\omega\tau_\mathrm{sf})$ with λ_sf being the spin diffusion length.

IV. CALCULATION OF THE LONGITUDINAL SPIN SEEBECK EFFECT

In this section we present a linear-response calculation of the longitudinal spin Seebeck effect and justify the phenomenological picture presented in Sec. II. The spin current I_s injected into N due to the longitudinal spin Seebeck effect is composed of three terms,

$$I_s = I_s(a) + I_s(b) + I_s(c), \tag{8}$$

where $I_s(a)$, $I_s(b)$, and $I_s(c)$ correspond to diagram (a), (b), and (c) in Fig. 2. Below we show that each term has the following sign:

$$I_s(a) < 0, \quad I_s(b) < 0, \quad I_s(c) > 0. \tag{9}$$

First, let us consider diagram (a). This can be calculated by setting $\underline{\check{X}}_{\boldsymbol{q}}(\omega) \to \check{X}_{\boldsymbol{q}}(\omega)$ and $\underline{\check{\chi}}_{\boldsymbol{k}}(\omega) \to \check{\chi}_{\boldsymbol{k}}(\omega)$ in Eq. (5), which was already done in Ref. [11] with the injected spin current given by (see Eq. (12) therein)

$$\begin{aligned} I_s(a) &= \frac{4N_\mathrm{int}J_\mathrm{sd}^2 S_0^2}{\sqrt{2}\hbar^2 N_N N_F} \sum_{\boldsymbol{q},\boldsymbol{k}} \int_\omega \mathrm{Im}\chi_{\boldsymbol{k}}^R(\omega)\mathrm{Im}X_{\boldsymbol{q}}^R(\omega) \\ &\quad \times \left[\coth(\tfrac{\hbar\omega}{2k_\mathrm{B}T_2}) - \coth(\tfrac{\hbar\omega}{2k_\mathrm{B}T_1})\right], \end{aligned} \tag{10}$$

where we have introduced the shorthand notation $\int_\omega = \int_{-\infty}^{\infty}\frac{d\omega}{2\pi}$, and N_int is the number of localized spins at the N/F interface. Note that $I_s(a)$ has a negative value due to $T_2 > T_1$.

Next, let us consider diagram (b). In this process, the localized spins in F is excited by the nonequilibrium phonon driven by the temperature gradient in F, hence this corresponds to the phonon-drag process [12]. Evaluation of the diagram was already given in Ref. [12], although the calculation is lengthy and tedious (see the supplemental material therein). In short, this term can be calculated by setting in Eq. (5) $\underline{\check{X}}_{\boldsymbol{q}}(\omega) \to \delta\check{X}_{\boldsymbol{q}}^{n\text{-}eq}(\omega) = \left(\begin{smallmatrix} 0, & \delta X_{\boldsymbol{q}}^{n\text{-}eq,K} \\ 0, & 0 \end{smallmatrix}\right)$ with its Keldysh component given by

$$\begin{aligned} \delta X_{\boldsymbol{q}}^{n\text{-}eq,K}(\omega) &= -2\sum_{\boldsymbol{K}} \frac{\Gamma_{\boldsymbol{K},\boldsymbol{q}}^2}{2N_F} \int_\nu \delta D_{\boldsymbol{K}}^{n\text{-}eq,K}(\nu)\mathrm{Im}X_{\boldsymbol{q}_-}^R(\omega_-) \\ &\quad \times |X_{\boldsymbol{q}}^R(\omega)|^2 \left[\coth(\tfrac{\hbar\omega_-}{2k_\mathrm{B}T_2})] - \coth(\tfrac{\hbar\omega}{2k_\mathrm{B}T_2})\right], \end{aligned} \tag{11}$$

where we have introduced shorthand notations $\omega_- = \omega - \nu$, $\boldsymbol{q}_- = \boldsymbol{q} - \boldsymbol{K}$, and $\int_\nu = \int_{-\infty}^{\infty}\frac{d\nu}{2\pi}$, and

$$\Gamma_{\boldsymbol{K},\boldsymbol{q}} = g_\mathrm{m-p}\sqrt{\frac{\hbar\nu_{\boldsymbol{K}}}{2M_\mathrm{ion}v_\mathrm{ph}^2}} \tag{12}$$

is the magnon-phonon interaction vertex. Here, $\nu_{\boldsymbol{K}}$, v_ph and M_ion are the phonon frequency, phonon velocity and the ion mass, respectively, and the strength of the magnon-phonon coupling is given by $g_\mathrm{m-p} = |a_S\boldsymbol{\nabla}J_\mathrm{ex}|(\omega_{\boldsymbol{q}}/J_\mathrm{ex})$ with the exchange interaction J_ex. In Eq. (11),

$$\begin{aligned} \delta D_{\boldsymbol{K}}^{n\text{-}eq,K}(\nu) &= 2i\sum_{\boldsymbol{K}'} \frac{|\Omega_\mathrm{ph}^{\boldsymbol{K}+\boldsymbol{K}'}|^2}{N_F^2}\mathrm{Im}D_{\boldsymbol{K}'}^R(\nu)|D_{\boldsymbol{K}}^R(\nu)|^2 \\ &\quad \times \left[\coth(\tfrac{\hbar\nu}{2k_\mathrm{B}T_3}) - \coth(\tfrac{\hbar\nu}{2k_\mathrm{B}T_2})\right] \end{aligned} \tag{13}$$

is the Keldysh component of the nonequilibrium phonon propagator. Here $\Omega_\mathrm{ph}^{\boldsymbol{K}+\boldsymbol{K}'}$ is the Fourier transform of $\Omega_\mathrm{ph}(\boldsymbol{r}) = \Omega_0 \sum_{\boldsymbol{r}_0 \in F/F\text{-interface}} a_S^3\delta(\boldsymbol{r} - \boldsymbol{r}_0)$ with $\Omega_0 =$

$\sqrt{2K_{\rm ph}/M_{\rm ion}}$, $K_{\rm ph}$ is the elastic constant, and a_S^3 is the cell volume of the ferromagnet. Putting these expressions into Eq. (5) and after some algebra, we finally obtain

$$I_s(b) = \frac{-L}{N_N N_F^3} \sum_{\boldsymbol{k,q,K,K'}} (\Gamma_{\boldsymbol{K,q}})^2 \int_\nu A_{\boldsymbol{k,q}}(\nu)|D_{\boldsymbol{K}}^R(\nu)|^2$$
$$\times {\rm Im} D_{\boldsymbol{K'}}^R(\nu) \big[\coth(\tfrac{\hbar\nu}{2k_{\rm B}T_3}) - \coth(\tfrac{\hbar\nu}{2k_{\rm B}T_2}) \big] \quad (14)$$

where $D_{\boldsymbol{K}}^R(\nu) = (\nu - \nu_{\boldsymbol{K}} + {\rm i}/\tau_{\rm ph})^{-1} - (\nu + \nu_{\boldsymbol{K}} + {\rm i}/\tau_{\rm ph})^{-1}$ is the retarded component of the phonon propagator with the phonon lifetime $\tau_{\rm ph}$, $L = \sqrt{2}(J_{sd}^2 S_0)\Omega_0^2 N_{\rm int} N'_{\rm int}/N_F$ with $N'_{\rm int}$ being the number of lattice sites at the F/F interface, and $A_{\boldsymbol{k,q}}(\nu)$ is defined by

$$A_{\boldsymbol{k,q}}(\nu) = \int_\omega {\rm Im}\chi_{\boldsymbol{k}}^R(\omega){\rm Im}X_{\boldsymbol{q_-}}^R(\omega_-)$$
$$\times |X_{\boldsymbol{q}}^R(\omega)|^2[\coth(\tfrac{\hbar\omega_-}{2k_{\rm B}T_2}) - \coth(\tfrac{\hbar\omega}{2k_{\rm B}T_2})]. \quad (15)$$

Note that only the even component of $A_{\boldsymbol{k,q}}(\nu)$ as a function of ν gives a non-vanishing contribution to Eq. (14). Because the even component of $A_{\boldsymbol{k,q}}(\nu)$ is negative definite as well as ${\rm Im}D_{\boldsymbol{K}}^R(\nu)[\coth(\tfrac{\hbar\nu}{2k_{\rm B}T_3}) - \coth(\tfrac{\hbar\nu}{2k_{\rm B}T_2})]$ in Eq. (14), $I_s(b)$ has a negative value.

Finally, let us consider diagram (c). Repeating essentially the same procedure in evaluating diagram (b), we obtain

$$I_s(c) = \frac{L'}{N_N N_F^3} \sum_{\boldsymbol{k,q,K,K'}} (\Upsilon_{\boldsymbol{K,k}})^2 \int_\nu B_{\boldsymbol{k,q}}(\nu)|\widetilde{D}_{\boldsymbol{K}}^R(\nu)|^2$$
$$\times {\rm Im} D_{\boldsymbol{K'}}^R(\nu) \big[\coth(\tfrac{\hbar\nu}{2k_{\rm B}T_2}) - \coth(\tfrac{\hbar\nu}{2k_{\rm B}T_1}) \big] \quad (16)$$

where $L' = \sqrt{2}(J_{sd}^2 S_0)\Omega_0^2 N_{\rm int}^2/N_F$, $\widetilde{D}_{\boldsymbol{K}}^R(\nu)$ denotes the phonon propagator in N. In the above equation, the coupling between the itinerant spin density and the phonon in N is given by

$$\Upsilon_{\boldsymbol{K,k}} \approx g_{\rm s-p}\sqrt{\frac{\hbar\nu_{\boldsymbol{K}}}{2M_{\rm ion}v_{\rm ph}^2}}, \quad (17)$$

where $g_{\rm s-p} \approx |a\boldsymbol{\nabla}t_{\rm hop}|U^2 N'(0)$ with a and $t_{\rm hop}$ being the lattice spacing and the hopping integral of the nonmagnetic metal N. In Eq. (16), $B_{\boldsymbol{k,q}}(\nu)$ is defined by

$$B_{\boldsymbol{k,q}}(\nu) = \int_\omega {\rm Im}\chi_{\boldsymbol{k}}^R(\omega){\rm Im}X_{\boldsymbol{q_-}}^R(\omega_-)|\chi_{\boldsymbol{q}}^R(\omega)|^2$$
$$\times [\coth(\tfrac{\hbar(\omega_-)}{2k_{\rm B}T_1}) - \coth(\tfrac{\hbar\omega}{2k_{\rm B}T_1})]. \quad (18)$$

Note that as in Eq. (14), only the even-in-ν component of $B_{\boldsymbol{k,q}}(\nu)$ gives non-vanishing contribution to Eq. (16). Then, because the even-in-ν component of $B_{\boldsymbol{k,q}}(\nu)$ is negative definite, $I_s(c)$ has a positive value.

V. DISCUSSION

In the previous section, we proved that $I_s(a)$ and $I_s(b)$ have the same sign, whereas $I_s(c)$ have the opposite sign

[Eq. (9)]. Then, if $I_s(c)$ is dominant in Eq. (8), it means that the sign of the longitudinal spin Seebeck effect can be opposite to that of the transverse spin Seebeck effect, since the sign of $I_s(a)$ and $I_s(b)$ is the same as that of the transverse spin Seebeck effect (see Refs. [11] and [12]). Because $I_s(a)$ and $I_s(b)$ are considered to have the same magnitude at room temperature (see Fig. 3 in Ref. [12]), we here compare the magnitude of $I_s(b)$ and $I_s(c)$.

The key quantities determining the magnitude of $I_s(b)$ and $I_s(c)$ are the interaction vertex $\Gamma_{\boldsymbol{K,q}}$ between magnons and phonons [solid circle in Fig. 2 and Eq. (12)] and the interaction vertex $\Upsilon_{\boldsymbol{K,k}}$ between spin accumulation and phonons [solid triangle in Fig. 2 and Eq. (17)]. The magnitude of these couplings is roughly given by $g_{\rm m-p} \approx |a_S\boldsymbol{\nabla}J_{\rm ex}|(\omega_{\boldsymbol{q}}/J_{\rm ex})$ and $g_{\rm s-p} \approx |a\boldsymbol{\nabla}t_{\rm hop}|U^2 N'(0)$, where a, $t_{\rm hop}$, U, $N'(0)$ are the lattice spacing, the hopping integral, the strength of the Coulomb repulsion, and the strength of the particle-hole asymmetry in the nonmagnetic metal N. For materials with a relatively large Coulomb repulsion U [18] and moderate strength of particle-hole asymmetry $N'(0)$ [19] such as Pt, we expect a situation $g_{\rm s-p} > g_{\rm m-p}$, which then explains the sign reversal of the spin injection signal in the longitudinal spin Seebeck effect due to Eqs. (8) and (9). From these considerations, we conclude that this happens in the longitudinal spin Seebeck effect reported in Refs. [6] and [7].

VI. CONCLUSION

In this paper we have developed linear-response theory of the longitudinal spin Seebeck effect. We have shown that the sign of the spin injection signal in the longitudinal spin Seebeck effect can be opposite to that in the conventional transverse spin Seebeck effect when the interaction between the spin accumulation and the phonon in the attached nonmagnetic metal is sufficiently stronger than the interaction between the magnon and the phonon in the ferromagnet. The linear-response approach presented in this paper can explain the sign reversal of the spin injection signal recently observed in the longitudinal spin Seebeck effect [6, 7].

Appendix A: Calculation of the vertex Υ

In this Appendix, we evaluate the interaction vertex $\Upsilon_{\boldsymbol{K,k}}$ (solid triangle in Fig. 2) between the itinerant spin density and the phonon in the nonmagnetic metal N. We
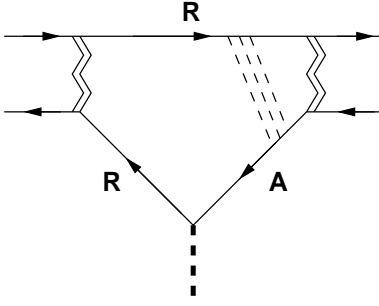
FIG. 3: Diagram corresponding to the interaction vertex $\Upsilon_{\boldsymbol{K},\boldsymbol{k}}$ between the itinerant spin density and the phonon. The solid line, the wavy line, the dashed line and the triple dashed line represent the electron propagator, the Coulomb repulsion, the phonon propagator, and the diffuson propagator, respectively. "R" or "A" means the retarded or advanced component of the electron Green's function.

assume that the nonmagnetic metal N has a moderately large Stoner enhancement factor, and for conduction electrons in N we use a model described by Ref. [17], and assume an elastic impurity scattering as well. The interaction vertex before integrating out the fermionic degrees

of freedom is shown in Fig. 3. The building block of this diagram is given by a triangle

$$\mathcal{T} = \int_{\epsilon}\left[\tanh(\tfrac{\hbar(\epsilon-\omega)}{2k_{\mathrm{B}}T}) - \tanh(\tfrac{\hbar\epsilon}{2k_{\mathrm{B}}T})\right]$$
$$\times \int_{\boldsymbol{p}}\mathrm{Im}G^{R}_{\boldsymbol{p}-\boldsymbol{k}}(\epsilon-\omega)G^{R}_{\boldsymbol{p}}(\epsilon)G^{A}_{\boldsymbol{p}}(\epsilon),\text{(A1)}$$

where $G^{R/A}_{\boldsymbol{p}}(\epsilon) = (\epsilon-\epsilon_{\boldsymbol{p}}\pm\mathrm{i}/\tau)^{-1}$ is the electron Green's function with the electron's lifetime τ. This diagram can be evaluated to be $\mathcal{T}\approx N'(0)\omega\tau$ as was done in Ref. [20]. After the inclusion of a diffuson vertex correction (triple dashed ladder in Fig. 3) which is important in a realistic diffusive situation, we obtain

$$\mathcal{T} \approx N'(0)\frac{(\omega\tau)^2}{(Dk^2\tau)^2 + (\omega\tau)^2},\tag{A2}$$

where D is the diffusion constant. The dominant contribution comes from the dynamical region $\omega\gg Dk^2$ and in this case we approximately have $\mathcal{T}\approx N'(0)$. By attaching two Coulomb repulsion U and one electron-phonon interaction $\approx|a\boldsymbol{\nabla}t_{\mathrm{hop}}|\sqrt{\frac{\hbar\nu_{\boldsymbol{K}}}{2M_{\mathrm{ion}}v_{\mathrm{ph}}^2}}$ [21] coming from each vertex, we finally obtain Eq. (17).

[1] G. E. W. Bauer, E. Saitoh, and B. J. van Wees, Nature Materials **11**, 391 (2012).
[2] K. Uchida, S. Takahashi, K. Harii, J. Ieda, W. Koshibae, K. Ando, S. Maekawa, and E. Saitoh Nature **455**, 778 (2008).
[3] S. Bosu, Y. Sakuraba, K. Uchida, K. Saito, T. Ota, E. Saitoh, and K. Takanashi, Phys. Rev. B **83**, 224401 (2011).
[4] C. M. Jaworski, J. Yang S. Mack, D. D. Awschalom, J. P. Heremans, and R. C. Myers, Nature Mater. **9**, 898 (2010).
[5] K. Uchida, J. Xiao, H. Adachi, J. Ohe, S. Takahashi, J. Ieda, T. Ota, Y. Kajiwara, H. Umezawa, H. Kawai, G. E. W. Bauer, S. Maekawa, and E. Saitoh, Nature Mater. **9**, 894 (2010).
[6] K. Uchida, H. Adachi, T. Ota, H. Nakayama, S. Maekawa, and E. Saitoh, Appl. Phys. Lett **97**, 172505 (2010).
[7] K. Uchida, T. Nonaka, T. Ota, H. Nakayama, and E. Saitoh, Appl. Phys. Lett **97**, 262504 (2010).
[8] S. Y. Huang, W. G. Wang, S. F. Lee, J. Kwo, and C. L. Chien, Phys. Rev. Lett. **107**, 216604 (2011).
[9] M. Weiler, M. Althammer, F. D. Czeschka, H. Huebl, M. S. Wagner, M. Opel, I. Imort, G. Reiss, A. Thomas, R. Gross, and S. T. B. Goennenwein, Phys. Rev. Lett. **108**, 106602 (2012).
[10] J. Xiao, G. E. W. Bauer, K. Uchida, E. Saitoh, and S. Maekawa, Phys. Rev. B **81**, 214418 (2010).
[11] H. Adachi, J. Ohe, S. Takahashi, and S. Maekawa, Phys. Rev. B **83**, 094410 (2011).
[12] H. Adachi, K. Uchida, E. Saitoh, J. Ohe, S. Takahashi, and S. Maekawa, Appl. Phys. Lett. **97**, 252506 (2010).
[13] H. Adachi and S. Maekawa, to appear in *Handbook of Spintronics* (Canopus Academic Publishing).
[14] G. A. Slack and D. W. Oliver DW, Phys. Rev. B 4, 592 (1971).
[15] A. I. Larkin and Yu. N. Ovchinnikov, *Zh. Eksp. Teor. Fiz.* **68**, 1915 (1975) [*Sov. Phys. JETP* **41**, 960 (1975)].
[16] Definition of the magnon propagator in this paper differs from that in Ref. [11] by a factor S_0.
[17] A. Kawabata, J. Phys. F: Metal Phys. **4**, 1477 (1974).
[18] Platinum is known to be a metal with moderately large Stoner enhancement. See, e.g., O. Gunnarsson, J. Phys. F: Metal Phys. **6**, 587 (1976).
[19] The Seebeck coefficent can be a measure of the particle-hole assymmetry. See J. P. Moore and R. S. Graves, J. Appl. Phys. **44**, 1174.
[20] A. Kamenev and Y. Oreg, Phys. Rev. B **52**, 7516 (1995).
[21] M. B. Walker, M. F. Smith, and K. V. Samokhin, Phys. Rev. B **65**, 014517 (2001).